AIAA'88

AIAA-88-0152

Third-Order Nonlinear Acoustic Instabilities in Combustion Chambers, Part II: Transverse Modes

V. Yang and S. I. Kim
The Pennsylvania State University
University Park, PA

F. E. C. Culick
California Inst. of Technology
Pasadena, CA

AIAA 26th Aerospace Sciences Meeting
January 11-14, 1988/Reno, Nevada

THIRD-ORDER NONLINEAR ACOUSTIC INSTABILITIES IN COMBUSTION CHAMBERS, PART II: TRANSVERSE MODES

Vigor Yang* and Seung-Ill Kim**
The Pennsylvania State University
University Park, Pennsylvania 16802

Fred E. C. Culick+
California Institute of Technology
Pasadena, California 91125

ABSTRACT

An analytical analysis has been developed to investigate the behavior of unsteady transverse pressure oscillations in combustion chambers. The model extends the previous analysis for the second-order standing wave motions and accommodates spinning oscillations and third-order nonlinearities. The influences of various parameters and initial conditions on the limit cycles and triggering of pressure oscillations are discussed. Results indicate that the existence of spinning oscillations depends strongly on the number of modes included in the analysis and on the initial conditions. The third-order acoustics has little influence on the triggering of instability. It only modifies the characteristics of limiting amplitudes.

1. INTRODUCTION

Unsteady motions excited and sustained by combustion processes are a fundamental problem in the development of high performance propulsion systems. The essential cause is the high rate of energy release confined to a volume in which energy losses are relatively small. Only a very small amount of chemical energy needs to be transformed to mechanical energy of time-varying fluid motions to produce unacceptable excursion of pressure oscillations. The ensuing vibrations of the structure may lead to failure of the structure itself or of equipment and instrumentation.

Two types of nonlinear instabilities have been commonly observed. They are classified as spontaneous and pulsed oscillations according to the mechanisms of initiation. Spontaneous instabilities require no external disturbances and arise from causes entirely internal to the system. Typically, a small unstable initial disturbance grows exponentially for some time, eventually reaching a limiting amplitude. Pulsed oscillation, also known as triggered instability, refers to initiation of instabilities by finite amplitude disturbance in a system which is otherwise stable to small perturbations. Instabilities occur only if the amplitude of initial disturbance exceeds certain critical value. Both spontaneous and pulsed instabilities necessarily involve nonlinear processes. It is impossible for a disturbance to be triggered to a limiting amplitude by linear processes alone. However, the form and order of nonlinearities for each case may be quite different.

There are two important questions of practical concern: What amplitudes will unstable oscillations reach, and what sort of initial disturbances will cause a linearly stable system to exhibit oscillations? Both are related to the fundamental behavior of a nonlinear system and can be translated as theoretical problems of general nature. The first deals with the conditions for the existence and stability of limit cycles, a matter previously addressed by the authors[1,2] by considering the second-order nonlinear acoustic interactions. The second is related to the triggering of combustion instabilities. It appears that in order to answer this question, nonlinear influences besides the second-order gasdynamics must be considered. The purpose of this paper is to develop a general framework within which the influences of the third-order acoustics on the unsteady transverse motions in a combustion chamber can be studied formally. In addition, the effects of various parameters and initial conditions on the existence of spinning waves are discussed in detail. The case of longitudinal wave motions has been given in a companion paper.[3]

Several analyses of nonlinear combustion instabilities have been carried out. Powell[4] considered pressure oscillations in liquid propellant rockets. With the aid of the methods of normal mode expansion and spatial averaging, he was able to derive a system of ordinary differential equations for the amplitude of each mode, which was then solved numerically. Kooker and Zinn[5] studied triggering in solid propellant rockets by solving numerically the conservation equations with various combustion response functions included. Powell, et al.[6] also employed a similar technique described in Ref.4 for investigation of pressure oscillations in solid propellant rockets. Recently, Levine and Baum[7-9] conducted extensive numerical studies of pulse triggered instability in solid rocket motors. The scheme is capable of describing multi-shock, steep-fronted type of instabilities in various tactical motors. Very good comparison between calculated and measured[10] wave motions was observed.

In spite of the significant progress made so far, these numerical works suffer a common difficiency.

* Assistant Professor of Mechanical Engineering, Member AIAA.
** Graduate Student, Ph.D. Candidate.
+ Professor of Jet Propulsion and Applied Physics, Fellow AIAA.

They provide detailed results for each special situation. Many cases must be calculated to perceive trend and to draw conclusions concerning general behavior. As an alternative, we resort to analytical approximate methods here. In the following sections, a general framework accommodating various linear and nonlinear processes is first developed, followed by detailed discussions of spinning transverse oscillations and the influences of the third-order acoustics on nonlinear transverse oscillations. The case of second-order standing transverse oscillations has been given elsewhere[2].

2. FORMULATION: SPATIAL AVERAGING

The nonlinear wave equation for the pressure can be constructed by suitably manipulating the conservation equations and the equation of state. The formulation extends the previous analysis for second-order nonlinear oscillations[2,11] and accommodates third-order nonlinearities. It contains broadly three parts. First, the conservation equations for a two-phase mixture of gas and solid particles are written in the following forms.

$$\frac{\partial \rho}{\partial t} + \vec{u} \cdot \nabla \rho = W \tag{2.1}$$

$$\rho \frac{\partial \vec{u}}{\partial t} + \rho \vec{u} \cdot \nabla \vec{u} = -\nabla p + \vec{F} \tag{2.2}$$

$$\frac{\partial p}{\partial t} + \gamma p \nabla \cdot \vec{u} = -\vec{u} \cdot \nabla p + P \tag{2.3}$$

The function W represents the mass conversion rate of condensed phases to gas per unit volume, $\vec{F}$ includes the force of interaction between the gas and condensed phases and the momentum transfer to the gas due to residual combustion, P is the sum of the heat release associated with chemical reaction and the energy transfer between two phases. The next step is to decompose all dependent variables into mean and time-varying parts. To simplyfy the derivation, we assume that the mean values do not vary with time.

$$\begin{aligned} \rho &= \bar{\rho} + \rho'(t, \vec{r}) \\ \vec{u} &= \bar{\vec{u}}(\vec{r}) + \vec{u}'(t, \vec{r}) \\ p &= \bar{p} + p'(t, \vec{r}) \end{aligned} \tag{2.4}$$

Now substitute (2.4) into (2.1)-(2.3), collect coefficients of like powers, and rearrange the results to produce the nonlinear wave equation with its boundary condition valid to third order.

$$\begin{aligned} \frac{\partial^2 p'}{\partial t^2} - \bar{a}^2 \nabla^2 p' &= h; \\ \vec{n} \cdot \nabla p' &= -f \end{aligned} \tag{2.5}$$

where $\bar{a}$ is the speed of sound. The functions h and f contain all linear and nonlinear influences of combustion, mean flow, and unsteady motions. Care must be exercised when treating the nonlinear terms. If the Mach number of the mean flow and the amplitude of the oscillation have the same order of magnitude, the contributions from the nonlinear acoustics can be treated separately. For convenience, the source term h is further written as

$$h = h_\mu + h_\varepsilon + h_{\varepsilon\varepsilon} + h_\nu \tag{2.6}$$

The subscripts μ, ε, $\varepsilon\varepsilon$, and ν represent respectively the linear processes, the second-order gasdynamics, the third-order gasdynamics, and all other nonlinear contributions from $\vec{F}'$ and P'. The explicit expressions for h_μ, h_ε, and h_ν are given in Ref. 11. The third-order acoustic term $h_{\varepsilon\varepsilon}$ is shown to be[14]

$$\begin{aligned} h_{\varepsilon\varepsilon} = &- \nabla \cdot [p'(\vec{u}' \cdot \nabla)\vec{u}'] \\ &+ \frac{\gamma - 1}{2\bar{\rho}\bar{a}^2} \nabla \cdot (p'^2 \frac{\partial \vec{u}'}{\partial t}) \end{aligned} \tag{2.7}$$

The couplings between mean flow variations and acoustic motions are not included, but can be treated in same manner.

The solutions of the wave equation (2.5) are approximated by a synthesis of the normal modes of the chamber, with unknown time-varying amplitudes.

$$\begin{aligned} p' &= \bar{p} \sum_{n=1}^{\infty} \eta_n(t) \psi_n(\vec{r}); \\ \vec{u}' &= \sum_{n=1}^{\infty} \frac{\dot{\eta}_n(t)}{\gamma k_n^2} \nabla \psi_n(\vec{r}) \end{aligned} \tag{2.8}$$

where the ψ_n is the normal mode function satisfying

$$\begin{aligned} \nabla^2 \psi_n + k_n^2 \psi_n &= 0; \\ \vec{n} \cdot \nabla \psi_n &= 0 \end{aligned} \tag{2.9}$$

The basis of this expansion is that many of the observed combustion instabilities are composed of several harmonic motions with mode shapes corresponding to the normal modes of the system. For a cylindrical chamber, ψ_n has either of the following forms;

$$\begin{aligned} \psi_n(\vec{r}) &= \cos k_l x \cos m\theta J_m(\kappa_{ms}) \\ \psi_n(\vec{r}) &= \cos k_l x \sin m\theta J_m(\kappa_{ms}) \end{aligned} \tag{2.10}$$

with

$$k_n^2 = k_l^2 + \kappa_{ms}^2$$

For a chamber of length L and radius R, having a rigid boundary, the eigenvalues for the wave numbers are $k_l = l\pi/L$ and the roots of the derivative of the Bessel function, $[dJ_m(\kappa_{ms} r)/dr]_{r=R} = 0$.

After substituting (2.8) into (2.5), multiplying the result by ψ_n, and integrating over the entire volume, we obtain the set of ordinary differential equations for the amplitude of each mode.

$$\ddot{\eta}_n + \omega_n^2 \eta_n = \epsilon F_n \tag{2.11}$$

where ϵ is a bookkeeping parameter representing the amplitude of pressure oscillation.

The forcing function F_n is

$$F_n = -\frac{\bar{a}^2}{\bar{p}E_n^2}\left[\iiint \psi_n h dv + \iint \psi_n f ds\right] \qquad (2.12)$$

and

$$E_n^2 = \iiint \psi_n^2 dv \qquad (2.13)$$

Thus, the problem comes down to solving the set (2.11) for the time-dependent amplitude, to give the evolution of the system subject to a specified initial condition.

If only the nonlinear contributions from the gas-dynamics are considered, F_n can be expressed to the third order as

$$\begin{aligned} F_n = &-\sum_i \left(D_{ni}\dot{\eta}_i + E_{ni}\eta_i\right) \\ &-\sum_i \sum_j \left(A_{nij}\dot{\eta}_i\dot{\eta}_j + B_{nij}\eta_i\eta_j\right) \\ &-\sum_i \sum_j \sum_m \left(R_{nijm}\dot{\eta}_i\dot{\eta}_j\eta_m + S_{nijm}\eta_i\eta_j\eta_m\right) \end{aligned} \qquad (2.14)$$

where D_{ni} and E_{ni} arise from linear processes, A_{nij} and B_{nij} represent the second-order nonlinear acoustics, and R_{nijm} and S_{nijm} are coefficients associated with the third-order nonlinear acoustics. The explicit formulas for A_{nij}, B_{nij}, R_{nijm}, S_{nijm} are given in Ref.14. Within the present representation of unsteady motions, the amplitude of acoustic wave is assumed to have the same order of magnitude of the Mach number of the mean flow. Consequently, the influences of the mean flow do not appear directly in the nonlinear terms.

3. METHOD OF TIME AVERAGING

An approximate solution technique using the method of time avering is developed to solve the equation (2.11) for the time-dependent behavior of each acoustic mode. This technique is based on the observation that most of the oscillations encountered in practical systems have amplitudes and frequencies which change relatively slowly during one period of oscillation. Thus the amplitudes are assumed to have the form,

$$\begin{aligned} \eta_n &= r_n(t)\sin(\omega_n t + \phi_n(t)) \\ &= A_n(t)\sin\omega_n t + B_n(t)\cos\omega_n t \end{aligned} \qquad (3.1)$$

where $r_n(t)$, $\phi_n(t)$, $A_n(t)$, $B_n(t)$ are slowly varying functions of time. After substituting in (2.11) and imposing the condition

$$\dot{A}_n \sin\omega_n t + \dot{B}_n \cos\omega_n t = 0, \qquad (3.2)$$

we obtain the following equations for $A_n(t)$ and $B_n(t)$.

$$\begin{aligned} \frac{dA_n}{dt} &= \frac{\epsilon}{\omega_n}F_n\cos\omega_n t \\ \frac{dB_n}{dt} &= -\frac{\epsilon}{\omega_n}F_n\sin\omega_n t \end{aligned} \qquad (3.3)$$

To facilitate analyses and to obtain the approximate solutions for A_n and B_n, we introduce two time scales, a fast scale $1/\omega_n$, proportional to the period of the oscillation; and a slow scale $1/\epsilon\omega_n$, which charaterizes the relatively gradual variations of the amplitude and phase. Correspondingly, the dimensionless fast and slow time variables are defined as $t_f = \omega_n t$ and $t_s = \epsilon\omega_n t$. Thus, equation (3.3) generally contain terms of the form shown below:

$$\frac{dA_n}{dt_s} = f_{n1}(t_s) + F_{n1}(t_f) + f_{n2}(t_s)F_{n2}(t_f) \qquad (3.4)a$$

$$\frac{dB_n}{dt_s} = g_{n1}(t_s) + G_{n1}(t_f) + g_{n2}(t_s)G_{n2}(t_f) \qquad (3.4)b$$

The explicit equations for A_n and B_n are given in Ref.14. These equations show explicitly that the right hand sides involve both fast and slowly varying processes, and A_n and B_n are slowly varying functions of time since t_s represents the slow time. For a small but finite interval in t_s and in the limit $\epsilon \to 0$, the corresponding interval in t_f is large. Thus, in the slow time scale the slowly varying functions, f_{ni} and g_{ni}, change slowly, but the fast varying functions, F_{ni} and G_{ni}, execute many oscillations. To first approximation, we may replace F_{ni} and G_{ni} by their time-mean quantities in the numerical integration of A_n and B_n[12]. Consequently, (3.4) becomes

$$\frac{dA_n}{dt_s} = f_{n1}(t_s) + \langle F_{n1}(t_f)\rangle + f_{n2}(t_s)\langle F_{n2}(t_f)\rangle \qquad (3.5)a$$

$$\frac{dB_n}{dt_s} = g_{n1}(t_s) + \langle G_{n1}(t_f)\rangle + g_{n2}(t_s)\langle G_{n2}(t_f)\rangle \qquad (3.5)b$$

where $\langle\ \rangle$ represents time-averaged quantity defined for a function $\psi(t_f)$ as

$$\langle\psi(t_f)\rangle = \lim_{T\to\infty}\frac{1}{T}\int_0^T \psi(t_f)dt_f$$

In summary, the method contains two steps: separation of the fast and slowly varying processes, and time average of the fast varying terms. For some practical problems, there is no clear distinction between fast and slowly varying terms. The numerical study of Yang, et al.[13] has shown that in order to both simplify the analysis and maintain good approximation, those terms with frequencies greater than one half of ω_n should be considered as fast-varying functions and be averaged.

4. NONLINEAR TRANSVERSE OSCILLATIONS

The theoretical model and the method of approximate solution disscussed in Sections 2 and 3 are used to investigate the third-order nonlinear transverse oscillations in a cylindrical combustion chamber. Compared with the longitudinal wave oscillations, the analysis for the transverse oscillations is much more complicated as a consequence of the peculiar normal mode frequencies. Owing to the analytical tractability, only the first three modes are considered here. The wave numbers and mode shapes are given below.

First Tangential Mode (1T)

$$\kappa_{11}R = 1.8412;$$
$$\psi_1 = \cos\theta J_1(\kappa_{11}R); \quad \psi_4 = \sin\theta J_1(\kappa_{11}R) \tag{4.1}a$$

First Radial Mode (1R)

$$\kappa_{01}R = 3.8317;$$
$$\psi_2 = J_0(\kappa_{01}R) \tag{4.1}b$$

Second Tangential Mode (2T)

$$\kappa_{21}R = 3.0542;$$
$$\psi_3 = \cos 2\theta J_2(\kappa_{21}R); \quad \psi_5 = \sin 2\theta J_2(\kappa_{21}R) \tag{4.1}c$$

To simplify writing we define $\kappa_1 = \kappa_{11}$, $\kappa_2 = \kappa_{01}$, and $\kappa_3 = \kappa_{21}$. The inclusion of both azimuthal eigenfunctions of tangential modes of oscillations allows the possibility of either standing and spinning waves, or a combination of both. In the following sections, spinning transverse oscillations are first examined within the second-order acoustics, followed by a discussion of the third-order transverse wave motions.

5. SPINNING TRANSVERSE OSCILLATIONS

Spinning transverse oscillations are commonly observed in many types of combustion chambers under a wide spectrum of environments. To fix ideas, we first consider a simple case with only the first tangential and the first radial modes taken into account.

5.1 The First Tangential / First Radial Modes

For spinning oscillations, each tangential mode contains two periodic motions in the azimuthal direction. The analysis therefore includes two mode functions, ψ_1 and ψ_4, for the first tangential mode, and one mode function, ψ_2, for the first radial mode, as defined by (4.1)a and (4.1)b respectively. As a first approach, the linear coupling terms between the two modes of the first tangential mode are neglected for simplicity, a reasonable assumption that holds in many practical cases. For example, one can show easily from the work of Culick[11] that the coefficients of linear coupling become zero if the mean flow velocity and the combustion response depend solely on axial position. Consequently, the linear parameters for the first tangential modes of oscillation satisfy the following relations:

$$\alpha_1 = \alpha_4 \quad \text{and} \quad \theta_1 = \theta_4 \tag{5.1}$$

With the aid of the time-averaging procedure described in section 3, we obtain the approximate equations for $A_n(t)$ and $B_n(t)$. To facilitate analysis, A_n and B_n are written in terms of amplitude and phase.

$$A_n(t) = r_n(t)\cos\phi_n(t),$$
$$B_n(t) = r_n(t)\sin\phi_n(t) \tag{5.2}$$

After substitution (5.2) in (3.5) written for two modes only and rearrangement of the result, we find the equations governing the wave amplitude and phase of each mode.

First Tangential Mode

$$\frac{dr_1}{dt} = r_1[\alpha_1 + a_1 r_2 \cos X] \tag{5.3}$$

$$\frac{dr_4}{dt} = r_4[\alpha_4 + a_1 r_2 \cos Y] \tag{5.4}$$

First Radial Mode

$$\frac{dr_2}{dt} = \alpha_2 r_2 + b_1[r_1^2\cos X + r_4^2\cos Y] \tag{5.5}$$

with

$$\frac{dX}{dt} = -2\theta_1 + \theta_2 + \Omega_1 - 2a_1 r_2 \sin X - \frac{b_1}{r_2}[r_1^2\sin X + r_4^2\sin Y] \tag{5.6}$$

$$\frac{dY}{dt} = -2\theta_4 + \theta_2 + \Omega_1 - 2a_1 r_2 \sin Y - \frac{b_1}{r_2}[r_1^2\sin X + r_4^2\sin Y] \tag{5.7}$$

where

$$X(t) = 2\phi_1 - \phi_2 + \Omega_1 t$$
$$Y(t) = 2\phi_4 - \phi_2 + \Omega_1 t$$
$$a_1 = 0.1570\left(\frac{\bar{a}}{R}\right)$$
$$b_1 = -0.1054\left(\frac{\bar{a}}{R}\right) \tag{5.8}$$
$$\Omega_1 = 2\omega_1 - \omega_2$$

Similar to the case of standing oscillations[2], we seek the limiting values of r_n and ϕ_n in the form given below,

$$r_{n0} = \text{constant} \tag{5.9}a$$
$$\phi_{n0} = \nu_n t + \zeta_n \tag{5.9}b$$

The subscript $(\,)_0$ denotes values in the limit cycle. Physically, ν_n and ζ_n represent the frequency modulation and the phase, respectively. In the limit cycle, the wave amplitude reaches constant. Thus, (5.3) and

(5.4) imply that the phases X_0 and Y_0 are constants as well. Now combine (5.8) and (5.9)b to give,

$$2\nu_1 - \nu_2 + (2\omega_1 - \omega_2) = 0 \qquad (5.10)a$$
$$2\nu_4 - \nu_2 + (2\omega_1 - \omega_2) = 0 \qquad (5.10)b$$

and

$$X_0 = 2\varsigma_1 - \varsigma_2; \qquad Y_0 = 2\varsigma_4 - \varsigma_2 \qquad (5.10)c$$

Substitution of (5.9) in (5.3)-(5.7) and rearrangement of the result lead to

$$\frac{\alpha_4}{\alpha_1} = \frac{\cos Y_0}{\cos X_0}$$

$$\theta_1 - \theta_4 + a_1 r_{20}[\sin X_0 - \sin Y_0] = 0$$

Since $\alpha_1 = \alpha_4$ and $\theta_1 = \theta_4$ in the situation considered here,

$$Y_0 = X_0 + 2m\pi, \quad m = 0, 1, \ldots \qquad (5.11)$$

From (5.10)c, we have

$$\varsigma_1 = \varsigma_4 + m\pi, \quad m = 0, 1, \ldots \qquad (5.12)$$

The two modes of the first tangential mode are either in phase or out of phase by 180 degrees. With this condition and suitable manipulation of (5.3)-(5.7), we obtain the wave amplitudes in the limit cycle.

$$r_{10}^2 + r_{40}^2 = \frac{\alpha_1\alpha_2}{a_1 b_1}\frac{1}{\cos^2(2\varsigma_1 - \varsigma_2)} \qquad (5.13)a$$

$$r_{20} = -\frac{\alpha_1}{a_1\cos(2\varsigma_1 - \varsigma_2)} \qquad (5.13)b$$

Because $a_1 b_1$ is less than zero, $\alpha_1\alpha_2$ must be negative in order that the right hand side of (5.13)a be positive. This is the necessary and sufficient condition for the existence of limit cycles. If one mode is linearly stable, then the other must be linearly unstable. The phase ς_n and the frequency modulation ν_n are given by,

$$\nu_1 = -\frac{\alpha_1\theta_2 + \alpha_2\theta_1 + \alpha_1(2\omega_1 - \omega_2)}{2\alpha_1 + \alpha_2} \qquad (5.14)$$

$$2\varsigma_1 - \varsigma_2 = \tan^{-1}\Big[\frac{(\omega_2 - \theta_2) - 2(\omega_1 - \theta_1)}{2\alpha_1 + \alpha_2}\Big] \qquad (5.15)$$

By assumption, the motion in the limit cycle is periodic and one phase is arbitrary. We may take advantage of this by setting $\varsigma_1 = 0$ to simplify the solution. Within the present representation of nonlinear behavior, the amplitude r_n and frequency modulation ν_n of limit cycles depend solely on the linear parameters α_n, θ_n, and ω_n. Figure 1 shows one example illustrating the existence of a limit cycle.

For the present case in which linear coupling terms are ignored, modes 1 and 4 have a phase difference of either 0 or 180 degrees. As a result, in the limit cycle, the spinning wave degenerates to a sum of standing waves. To see this, we substitute (3.1) and (4.1) in (2.8), and use (5.12) to determine the acoustic pressure:

$$\begin{aligned} p'(\vec{r},t)/\bar{p} = {} & r_{10}\sin[(\omega_1 + \nu_1)t + \varsigma_1]\cos\theta J_1(k_1 r) \\ & \pm r_{40}\sin[2(\omega_1 + \nu_1)t + \varsigma_1]\sin\theta J_1(k_1 r) \\ & + r_{20}\sin[2(\omega_1 + \nu_1)t + \varsigma_2]J_0(k_2 r) \end{aligned} \qquad (5.16)$$

The first two terms of the right hand side can be further combined to give

$$\begin{aligned} p'(\vec{r},t)/\bar{p} = {} & \sqrt{r_{10}^2 + r_{40}^2}\sin[(\omega_1 + \nu_1)t + \varsigma_1]\times \\ & \cos(\theta \mp \phi_1)J_1(k_1 r) \\ & + r_{20}\sin[2(\omega_1 + \nu_1)t + \varsigma_2]J_0(k_2 r) \end{aligned} \qquad (5.17)$$

where $\phi_1 = \tan^{-1}(r_{40}/r_{10})$

The spatial- and time-dependent parts of each mode are separated, so they are standing waves. Note that the spatial angle ϕ_1 cannot be uniquely determined since the relative magnitudes of r_{10} and r_{40} are not known. Only the wave amplitudes can be calculated by (5.13)a,b. Figure 2 shows the time traces of pressure oscillations at various positions in the limit cycle with the linear parameters and the initial conditions specified by Figure 1. The results of pure standing modes are also included for comparison. The wave motion may have either larger or smaller amplitude, depending on the azimuthal position.

We have so far considered only the existence of limit cycles. The remaining task is to determine the conditions under which the limit cycle is stable. The procedure consists in examining small perturbations in the vicinity of the limit cycle. We set $r_n = r_{n0} + r_n'$, etc., the primed quantity being assumed small, substitute in (5.3)-(5.7), and neglect the higher-order terms to produce a system of linearized equations. The solutions vary exponentially in time and may be written in the form $r_1' = \tilde{r}_1\exp(\lambda t)$, ect. This leads to a system of linear algebraic equations for $\tilde{r}_n, \tilde{X}$, and $\tilde{Y}$, and its characteristic polynomial in λ has the form

$$P(\lambda) = (2\alpha_1 - \lambda)\lambda(\lambda^3 + P_1\lambda^2 + P_2\lambda + P_3) = 0 \qquad (5.18)$$

where

$$P_1 = -2(\alpha_1 + \alpha_2) \qquad (5.19)a$$
$$P_2 = \alpha_2[\alpha_2 - (4\alpha_1 - \alpha_2)\tan^2 X_0] \qquad (5.19)b$$
$$P_3 = 2\alpha_1\alpha_2(2\alpha_1 + \alpha_2)(1 + \tan^2 X_0) \qquad (5.19)c$$

Since $X_0 = Y_0$ in the limit cycle, two cases must be differentiated, depending on the phase relation between X' and Y'. If $X' = Y'$, the initial phase difference between the first and the fourth modes being 0 or 180 degrees, the characteristic equation (5.18) reduces to

$$P(\lambda) = \lambda^3 + P_1\lambda^2 + P_2\lambda + P_3 = 0 \qquad (5.20)$$

In order for the limit cycle to be stable, all roots of $P(\lambda)$ must have negative real parts. The necessary and

sufficient conditions for this to be true are commonly known as Routh-Hurwitz criteria:

$$P_1 > 0, \quad P_3 > 0, \quad P_1P_2 - P_3 > 0 \tag{5.21}$$

The first two inequalities together with the condition for existence give directly

$$\alpha_1 + \alpha_2 < 0 \tag{5.22}a$$
$$2\alpha_1 + \alpha_2 < 0 \tag{5.22}b$$
$$\alpha_1\alpha_2 < 0 \tag{5.22}c$$

The last inequality in (5.21) is more difficult to simplify. With some manipulations, we can show that for positive α_1 this condition is fully compatible with the inequalities (5.22)a-c, but it requires a stricter stability domain for negative α_1. For $\alpha_1 < 0$, the inequality reduces to

$$\alpha_1 > \frac{-|k|}{2+\xi}\sqrt{\frac{-\xi^2+2\xi+2}{\xi^2+2\xi+2}} \tag{5.23}$$

where $\xi = \alpha_2/\alpha_1$, $k = 2\theta_1 - \theta_2 - (2\omega_1 - \omega_2)$, and ξ is confined to the range $1 - \sqrt{3} < \xi < 0$.

The overall result for $k = 0.25$ is sketched in Figure 3, where the shaded regions represent stable limit cycles. Thus, stable limit cycles exist only if the first mode is linearly unstable and the second mode is stable with decay constant greater than twice the growth constant of the first, or if the first mode is linearly stable and the ratio of growth constants, α_2/α_1, satisfies the condition (5.23).

If the initial phase difference between the first and the fourth modes is neither 0 nor 180 degrees, i.e., $X' \neq Y'$, one has to use (5.18) to analyze the stability behavior of the limit cycle. For this case, the Routh-Hutwitz criteria require another condition

$$\alpha_1 < 0 \tag{5.24}$$

in addition to the conditions given by (5.21). Thus, stable limit cycles exist only if the first mode is linearly stable and (5.23) is satisfied.

Figure 4 shows an example of an unstable limit cycle in which the initial phase difference between modes 1 and 4 is 90 degrees. The linear parameters are the same as those for the stable limit cycle shown in Figure 1. The first tangential mode grows rapidly, while the first radial decays to zero. Figure 5 shows the existence of a stable limit cycle. Same as the case shown in Fig. 4, the initial phase difference $\phi_1 - \phi_4$ is 90 degrees, but the linear parameters satisfy the Routh-Hurwitz criteria.

Extensive numerical calculations have also been carried out to investigate the effects of linear coupling on the characteristics of limiting cycles. No conclusive results and explicit formulas are obtained at this point as a result of formidable algebra. Figure 6 shows a typical set of the time traces of η_n in a limit cycle. Both the amplitudes and phases of modes 1 and 4 of the first tangential mode are different. However, their frequencies remain the same and equal to one half of the first radial mode frequency. The time evolution of the amplitudes are;

First Tangential Mode

$$\eta_1(t) = r_{10}\sin[(\omega_1 + \nu_1)t] \tag{5.25}$$

$$\eta_4(t) = r_{40}\sin[(\omega_1 + \nu_1)t + \varsigma_4] \tag{5.26}$$

First Radial Mode

$$\eta_2(t) = r_{20}\sin[2(\omega_1 + \nu_1)t + \varsigma_2] \tag{5.27}$$

The phase of the first mode is taken to be zero, $\varsigma_1 = 0$. Now substitute the above equations in (2.3) and rearrange the result to give the pressure oscillation.

$$\begin{aligned} p' =& \{r_{10}\sin[(\omega_1+\nu_1)t+\theta] \\ &+ \sqrt{r_{10}^2 + r_{40}^2 - 2r_{10}r_{40}\sin\varsigma_4}\times \\ &\sin[(\omega_1+\nu_1)t+\phi]\sin\theta\}J_1(\kappa_1 r) \\ &+ r_{20}\sin[2(\omega_1+\nu_1)t+\varsigma_2]J_0(\kappa_2 r) \end{aligned} \tag{5.28}$$

where

$$\phi = \tan^{-1}\frac{r_{40}\sin\varsigma_4 - r_1}{r_{40}\cos\varsigma_4}$$

The first and second terms in the bracket stand for pure spinning and standing wave motions, respectively. If modes 1 and 4 are in phase, i.e., $\varsigma_4 = 0$, the first tangential mode degenerates to a standing wave and its pressure becomes

$$\begin{aligned} p' =& \sqrt{r_{10}^2 + r_{40}^2}\sin[(\omega_1+\nu_1)t]\times \\ &\sin(\theta-\phi)J_1(\kappa_1 r) \end{aligned} \tag{5.29}$$

Since it is the linear coupling which causes a nonzero phase ς_4, the result suggests that linear coupling is essential in establishing spinning wave motions for the first tangential/ first radial modes.

5.2 The First Tangential/Second Tangential Modes

The analysis of the first tangential/second tangential modes of spinning oscillations follows the same approach as that for the first tangential/ first radial modes. For direct comparison, we ignore the linear coupling terms and assume the following relations for the linear parameters:

$$\begin{aligned} &\alpha_1 = \alpha_4; \quad \theta_1 = \theta_4 \quad \text{and} \\ &\alpha_3 = \alpha_5; \quad \theta_3 = \theta_5 \end{aligned} \tag{5.30}$$

The approximate equations for $r_n(t)$ and $\phi_n(t)$ thus become

First Tangential Mode

$$\frac{dr_1}{dt} = \alpha_1 r_1 + a_2[r_1 r_3\cos X + r_4 r_5\cos Z] \tag{5.31}$$

$$\frac{dr_4}{dt} = \alpha_4 r_4 + a_2[r_1 r_5 \cos Z - r_3 r_4 \cos Y] \quad (5.32)$$

Second Tangential Mode

$$\frac{dr_3}{dt} = \alpha_3 r_3 + b_2[r_1^2 \cos X - r_4^2 \cos Y] \quad (5.33)$$

$$\frac{dr_5}{dt} = \alpha_5 r_5 + 2b_2 r_1 r_4 \cos Z \quad (5.34)$$

and

$$\begin{aligned}\frac{dX}{dt} =& -2\theta_1 + \theta_3 + \Omega_2 \\ & - \frac{1}{r_3}[2a_2 r_3^2 + b_2 r_1^2]\sin X \\ & + b_2\frac{r_4^2}{r_3}\sin Y - 2a_2\frac{r_4 r_5}{r_1}\sin Z\end{aligned} \quad (5.35)$$

$$\begin{aligned}\frac{dY}{dt} =& -2\theta_4 + \theta_3 + \Omega_2 \\ & + \frac{1}{r_3}[2a_2 r_3^2 + b_2 r_4^2]\sin Y \\ & - b_2\frac{r_1^2}{r_3}\sin X - 2a_2\frac{r_1 r_5}{r_4}\sin Z\end{aligned} \quad (5.36)$$

$$\begin{aligned}\frac{dZ}{dt} =& -\theta_1 - \theta_4 + \theta_5 + \Omega_2 \\ & - a_2 r_3[\sin X - \sin Y] \\ & - [a_2(\frac{r_1 r_5}{r_4} + \frac{r_4 r_5}{r_1}) + 2b_2\frac{r_1 r_4}{r_5}]\sin Z\end{aligned} \quad (5.37)$$

where

$$\begin{aligned}X(t) =& 2\phi_1 - \phi_3 + \Omega_2 t \\ Y(t) =& 2\phi_4 - \phi_3 + \Omega_2 t \\ Z(t) =& \phi_1 + \phi_4 - \phi_5 + \Omega_2 t \\ a_2 =& -0.0521(\frac{\bar{a}}{R}) \\ b_2 =& 0.1873(\frac{\bar{a}}{R}) \\ \Omega_2 =& 2\omega_1 - \omega_3\end{aligned} \quad (5.38)$$

In the limit cycle, the time derivatives drop and the above equations become a system of algebraic equations. In general, no unique solution can be found due to its peculiar structure. The solution may lead to standing or spinning wave motions, depending on the initial conditions. To elaborate this point, we consider two extreme cases. The first case deals with standing mode of oscillation. One can easily show that if $r_4 = r_5 = 0$ initially, (5.31) - (5.37) degenerate to the equations for r_1 and r_3 only, and the results for standing wave motions can be directly related to this case. The second case is concerned with simple spinning waves. By taking

$$\begin{aligned}\varsigma_4 = \varsigma_1 + \pi/2; \quad \varsigma_5 = \varsigma_3 + \pi/2 \\ r_{40} = r_{10}; \quad r_{50} = r_{30}\end{aligned} \quad (5.39)$$

Some manipulations of the governing equations give the solution for the amplitude and frequency modulation of each mode.

$$r_{10}^2 = \frac{\alpha_1\alpha_3}{4a_2 b_2}\frac{1}{\cos^2(2\varsigma_1 - \varsigma_3)} \quad (5.40)$$

$$r_{30} = -\frac{\alpha_1}{2a_2\cos(2\varsigma_1 - \varsigma_3)} \quad (5.41)$$

$$\nu_1 = -\frac{\alpha_1\theta_3 + \alpha_3\theta_1 + \alpha_1(2\omega_1 - \omega_3)}{2\alpha_1 + \alpha_3} \quad (5.42)$$

and

$$2\varsigma_1 - \varsigma_3 = \tan^{-1}[\frac{\omega_3 - 2\omega_1 + (\theta_3 - 2\theta_1)}{2\alpha_1 + \alpha_3}] \quad (5.43)$$

Now combine (2.8), (3.1), and (5.2), and use (5.30) to give the pressure oscillation of the first tangential/second tangential spinning wave motion.

$$\begin{aligned}p'/\bar{p} =& r_{10}\sin[(\omega_1 + \nu_1)t + \varsigma_1 + \theta]J_1(\kappa_1 r) \\ & + r_{30}\sin[2(\omega_1 + \nu_1)t + \varsigma_3 + 2\theta]J_2(\kappa_3 r)\end{aligned} \quad (5.44)$$

The analysis for the general case is much more complicated. After considerable manipulation of (5.31)-(5.37), we can express the limiting wave amplitudes in terms of the phase difference X_0, Y_0, and Z_0. Within the present treatment of acoustic waves, the solution contains two branches which represent respectively spinning and standing modes of oscillations. The remaining task is to determine the conditions under which a specific wave pattern may occur. This is related to the fundamental behavior of a nonlinear system subject to a given initial condition. To address this issue, a detailed analysis of (5.31)-(5.38) is carried out with a wide variety of initial conditions.[14] Results indicate clearly that spinning waves can be established only if the two modes of each tengential wave have an initial phase difference of 90 degrees, and the linear parameters satisfy the stability criteria given by (5.22) and (5.23). All other conditions give standing waves. Figures 7 through 9 are three examples illustrating the limiting behavior of the first tangential/second tangential wave motions at various azimuthal positions. The corresponding initial conditions are given below.

Case1 ($\phi_1 = \phi_3 = 0$ and $\phi_4 = \phi_5 = 0$ at $t = 0$)

1T Mode	$A_1(0) = 0.01$	$B_1(0) = 0$
	$A_4(0) = 0$	$B_4(0) = 0$
2T Mode	$A_3(0) = 0.01$	$B_3(0) = 0$
	$A_5(0) = 0$	$B_5(0) = 0$

Case2 ($\phi_1 = \phi_3 = 0$ and $\phi_4 = \phi_5 = \frac{\pi}{2}$ at $t = 0$)

1T Mode	$A_1(0) = 0.01$	$B_1(0) = 0$
	$A_4(0) = 0.01\cos\frac{\pi}{2}$	$B_4(0) = 0.01\sin\frac{\pi}{2}$
2T Mode	$A_3(0) = 0.01$	$B_3(0) = 0$
	$A_5(0) = 0.01\cos\frac{\pi}{2}$	$B_5(0) = 0.01\sin\frac{\pi}{2}$

Case3 ($\phi_1 = \phi_3 = 0$ and $\phi_4 = \phi_5 = \frac{\pi}{4}$ at $t = 0$)

1T Mode	$A_1(0) = 0.01$	$B_1(0) = 0$
	$A_4(0) = 0.01\cos\frac{\pi}{4}$	$B_4(0) = 0.01\sin\frac{\pi}{4}$
2T Mode	$A_3(0) = 0.01$	$B_3(0) = 0$
	$A_5(0) = 0.01\cos\frac{\pi}{4}$	$B_5(0) = 0.01\sin\frac{\pi}{4}$

To facilitate comparison, the initial phases of modes 1 and 3 are set to be zero for all three cases. Case 1 shows a degenerated standing wave with the initial values of A_n and B_n (n=4,5) equal to zero. The acoustic field has essentially a standing wave pattern, given node points at $\theta = (2n+1)\pi/2$ for the first tangential mode and $\theta = (2n+1)\pi/4$ for the second tangential mode. Case 2 has an initial phase difference of 90 degrees for both modes 1 and 4 and modes 3 and 5, respectively. A simple spinning oscillation is clearly seen for each tangential mode. The waves propagate harmonically in the azimuthal direction and no node point is observed. The last case shows a typical result of the general situation with the initial phases $\phi_4, \phi_5 \neq \frac{\pi}{2}, \frac{3\pi}{2}$. The waves have the same pattern as that for the first case, but the phases are different.

5.3 The First Tangential/First Radial /Second Tangential Modes

Spinning oscillations of the first three transverse modes are also investigated using the same analysis for the two-mode cases, but the algebra is much more complicated. There are ten independent equations for ten unknowns. To save space, only some important results are summarized here. Detailed discussion of this matter is given in Ref.14.

Unlike the case of the first tangential/second tangential modes in which stable spinning oscillations exist only if the initial phase differences, $\phi_1 - \phi_4$ and $\phi_3 - \phi_5$, are 90 degrees, the existence of three-mode spinning oscillations seems to be independent of the initial conditions. Spinning oscillations are always observed as long as the linear parameters satisfy the stability criteria. Figure 10 shows a typical example illustrating the existence of limit cycle. The initial phase difference between the two modes of each tangential mode is 90 degrees. The first and second tangential modes grow for a short while and then reach their limiting conditions. However, the first radial mode decreases to zero. Figure 11 shows the time traces of the wave amplitudes at various azimuthal positions. The waves propagate harmonically, suggesting the presence of spinning motions.

6. THIRD-ORDER TRANSVERSE OSCILLATIONS

The effects of third-order acoustics on transverse oscillations have been studied under the framework discussed in Sec.2 and 3. To fix ideas and to demonstrate its influences, only two modes are considered here.

6.1 First Tangential/ First Radial Modes.

The coupling between the first tangential and the first radial modes represents the simplest case and serve as the basis of analyzing transverse acoustic oscillations. Following the idea discussed in Sec.3, the fast varying terms with frequencies greater than one half of ω_n are averaged with respect to time. Therefore, the equations governing the amplitude and phase of each mode become

$$\begin{aligned}\frac{dr_1}{dt} =& \alpha_1 r_1 + a_1 r_1 r_2 \cos(2\phi_1 - \phi_2 + \Omega_1 t) \\ &+ \xi_3 r_1^3 \sin 2\phi_1 + r_1 r_2^2 (\xi_4 \sin 2\phi_1 \\ &+ \xi_1 \sin 2\phi_2 + \xi_2 \sin 2(\phi_1 - \phi_2))\end{aligned} \tag{6.1}$$

$$\begin{aligned}\frac{dr_2}{dt} =& \alpha_2 r_2 + b_1 {r_1}^2 \cos(2\phi_1 - \phi_2 + \Omega_1 t) \\ &+ \eta_3 r_2^3 \sin 2\phi_2 + r_1^2 r_2 (\eta_4 \sin 2\phi_1 \\ &+ \eta_1 \sin 2\phi_2 + \eta_2 \sin 2(\phi_1 - \phi_2))\end{aligned} \tag{6.2}$$

$$\begin{aligned}\frac{d\phi_1}{dt} =& -\theta_1 - a_1 r_2 \sin(2\phi_1 - \phi_2 + \Omega_1 t) \\ &+ r_1^2[-\xi_5 + (2\xi_5 - \xi_3)\cos 2\phi_1)] \\ &+ r_2^2[-\xi_6 + \xi_4 \cos 2\phi_1 - \xi_1 \cos 2\phi_2 \\ &+ \xi_2 \cos 2(\phi_1 - \phi_2)]\end{aligned} \tag{6.3}$$

$$\begin{aligned}\frac{d\phi_2}{dt} =& -\theta_2 + b_1 \frac{r_1^2}{r_2} \sin(2\phi_1 - \phi_2 + \Omega_1 t) \\ &+ r_1^2[\eta_6 - \eta_4 \cos 2\phi_1 + \eta_1 \cos 2\phi_2 \\ &- \eta_2 \cos 2(\phi_1 - \phi_2)] \\ &+ r_2^2[-\eta_5 + (2\eta_5 - \eta_3)\cos 2\phi_2)]\end{aligned} \tag{6.4}$$

where the coefficients ξ_n and η_n are given in Ref.14.

Unlike the case of the second-order acoustics, the set of (6.1)-(6.4) prohibits simple analytical analysis due to its rich frequency content. As an alternative, we resort to numerical integrations. Figure 12 shows a typical example illustrating the existence of limit cycle, where the dash and solid lines represent results based on the second and third-order nonlinear acoustic models, respectively. Compared with the second-order analysis, the third-order acoustics not only modifies the magnitude of oscillations, but also causes the modulation of amplitudes. The wave amplitudes vary periodically and contain many harmonics. It is interesting to note that for this particular case with $\theta_1 = \theta_2 = 0$, the wave amplitude of each mode oscillates with the same frequency and phase, a phenomenon requiring further exploration in the future. Figure 13 shows the time histories of the derivatives of phases, $d\phi_1/dt$ and $d\phi_2/dt$. Similar to the wave amplitudes, the phases also vary periodically, and they have the same frequency as that of the amplitudes. If we only consider the dominant fundamental harmonic, both the wave

amplitudes and phases have the following form.

$$\begin{aligned} r_1 &= r_{10} + r_{11}\sin(a_1 t + c_1); \\ r_2 &= r_{20} + r_{21}\sin(a_1 t + c_1); \\ \frac{d\phi_1}{dt} &= \nu_{10} + \nu_{11}\sin(a_1 t + c_2); \\ \frac{d\phi_2}{dt} &= \nu_{20} + \nu_{21}\sin(a_1 t + c_2); \end{aligned} \tag{6.5}$$

Now substitute the above expressions in (3.1) to obtain the time evolution of the acoustic modes.

$$\eta_1(t) = [r_{10} + r_{11}\sin(a_1 t + c_1)] \times \sin[(\omega_1 + \nu_{10})t - \frac{\nu_{11}}{a_1}\cos(a_1 t + c_2) + \zeta_1] \tag{6.6a}$$

$$\eta_2(t) = [r_{20} + r_{21}\sin(a_1 t + c_1)] \times \sin[(\omega_2 + \nu_{20})t - \frac{\nu_{21}}{a_1}\cos(a_1 t + c_2) + \zeta_2] \tag{6.6b}$$

The wave motions involve both amplitude and frequency modulations.

Figure 14 shows the time traces of η_1 and η_2. The presence of amplitude modulation due to the third-order nonlinearity is clearly seen. Figure 15 shows the enlarged time traces. Results indicate that the first radial mode oscillates at twice the frequency of the first tangential mode, a conclusion which is true for both the second-order and the third-order acoustic models.

In order to study the triggering phenomenon in the sense of stable limit cycle, the stability characteristics in the neighborhood of the trivial solution must be examined. Extensive numerical results indicate that for $\alpha_1 < 0$ and $\alpha_2 < 0$, the wave amplitude always decays in time to zero. Cosequently, we may conclude that the inclusion of the third-order acoustics only modifies the limiting behavior of oscillations, and it does not change the fundamental conditions for the existence and stability of limit cycles. The nonlinear gasdynamics simply serves as a means of transfer of energy between modes. It does not contribute to the growth or decay of the wave, even with the third-order nonlinearities included.

6.2 First Tangential/ Second Tangential Modes.

The equations governing this case are the same as those treated above, but the characteristics of the limit cycle differ because of the difference between the frequencies of the first radial and second tangential modes. The equations for the wave amplitude and phase have the following form.

$$\begin{aligned} \frac{dr_1}{dt} &= \alpha_1 r_1 + a_2 r_1 r_3 \cos(2\phi_1 - \phi_3 + \Omega_2 t) \\ &\quad + \Gamma_3 r_1^3 \sin 2\phi_1 + r_1 r_3^2 (\Gamma_4 \sin 2\phi_1 \\ &\quad + \Gamma_1 \sin 2\phi_3 + \Gamma_2 \sin 2(\phi_1 - \phi_3)) \end{aligned} \tag{6.7}$$

$$\begin{aligned} \frac{dr_3}{dt} &= \alpha_3 r_3 + b_2 {r_1}^2 \cos(2\phi_1 - \phi_3 + \Omega_2 t) \\ &\quad + \Lambda_3 r_3^3 \sin 2\phi_3 + r_1^2 r_3 (\Lambda_4 \sin 2\phi_1 \\ &\quad + \Lambda_1 \sin 2\phi_3 + \Lambda_2 \sin 2(\phi_1 - \phi_3)) \end{aligned} \tag{6.8}$$

$$\begin{aligned} \frac{d\phi_1}{dt} &= -\theta_1 - a_2 r_3 \sin(2\phi_1 - \phi_3 + \Omega_1 t) \\ &\quad + r_1^2[-\Gamma_5 + (2\Gamma_5 - \Gamma_3)\cos 2\phi_1)] \\ &\quad + r_3^2[-\Gamma_6 + \Gamma_4 \cos 2\phi_1 - \Gamma_1 \cos 2\phi_3 \\ &\quad + \Gamma_2 \cos 2(\phi_1 - \phi_3)] \end{aligned} \tag{6.9}$$

$$\begin{aligned} \frac{d\phi_3}{dt} &= -\theta_3 + b_2 \frac{r_1^2}{r_3} \sin(2\phi_1 - \phi_3 + \Omega_2 t) \\ &\quad + r_1^2[\Lambda_6 - \Lambda_4 \cos 2\phi_1 + \Lambda_1 \cos 2\phi_3 \\ &\quad - \Lambda_2 \cos 2(\phi_1 - \phi_3)] \\ &\quad + r_3^2[-\Lambda_5 + (2\Lambda_5 - \Lambda_3)\cos 2\phi_3)] \end{aligned} \tag{6.10}$$

The coefficients Γ_n and Λ_n are given in Ref.14.

Figure 16 shows the time history of a 1T/2T mode oscillation with the same values of linear parameters used for Figure 12. The amplitudes of η_1 and η_3 reach considerably larger values and contain many harmonics.

7. CONCLUSION

An analytical analysis has been constructed to investigate the behavior of nonlinear transverse oscillations. The influences of various parameters and initial conditions on the existence and stability of limit cycles were studied in detailed. Results indicate that for two-mode oscillations, spinning waves exist only if the initial phase difference between modes and the linear parameters satisfy some restrictive requirements. However, the dependence on the initial conditions is much relaxed in the case of three modes. The third-order nonlinear acoustics has also been investigated. While the third-order acoustics affects the limiting behavior of oscillations, it has little influence on the triggering of combustion instability.

ACKNOWLEDGEMENTS

This work was supported partly by the ONR Grant No. 00014-84-K-0434, and partly by The Pennsylvania State University. The authors are greatly indebted to Dr. H. S. Sun for his assistance in formulating the model of the third-order nonlinear acoustic model.

REFERENCES

1. Awad, E. and Culick, F. E. C., "On the Existence and Stability of Limit Cycles for Longitudinal Acoustic Modes in a Combustion Chamber," Combustion Science and Technology, Vol 46, 1986, PP. 195-222.
2. Yang, V. and Culick, F. E. C., "On the Existence and Stability of Limit Cycles for Transverse Acoustic Modes in a Combustion Chamber, Part I: Standing Modes," to be published.

3. Yang, V., Kim, S. I. and Culick, F. E. C., "Third-Order Nonlinear Acoustic Waves and Triggering of Pressure Oscillations in Combustion Chambers, Part I: Longitudinal Modes," AIAA Paper 87-1873, 1987.
4. Powell, E. A., "Application of the Galerkin Method in the Solution of Combustion Instability Problems," Ph.D. Thesis, Georgia Institute of Technology, 1970.
5. Kooker, D. E. and Zinn, B. T., "Triggering of Axial Instabilities in Solid Rockets: Numerical Predictions," AIAA Paper 73-1298, 1973.
6. Powell, E. A., Padmanabhan, M. S., and Zinn, B. T., "Approximate Nonlinear Analysis of Solid Rocket Motors and T-Burners," AFRPL-TR-77, Vol. 2, 1977.
7. Levine, J. N. and Baum, J. D., "A Numerical Study of Nonlinear Instabilities in Solid Rocket Motors," AIAA Journal, Vol. 21, 1982, PP. 557-564.
8. Baum, J. D., Lovine, R. L. and Levine, J. N., "Pulsing Techniques for Solid-Propellant Rocket Motors: Modeling and Cold-Flow Testing," Journal of Spacecraft, Vol. 20, 1983, PP. 150-157.
9. Lovine, R. L., Baum, J. D. and Levine, J. N., "Ejecta Pulsing of Subscale Solid Propellant Rocket Motors," AIAA Journal, Vol. 23, 1985, PP. 416-423.
10. Lovine, R. L. and Micheli, P. L., "Nonlinear Stability for Tactical Motors," AFRPL-TR-85-017, 1985.
11. Culick, F. E. C., "Nonlinear Behavior of Acoustic Waves in Combustion Chamber," Acta Astronautica, Vol. 3, 1976, pp. 715-734.
12. Culick, F. E. C. and Yang, V., "Theories of Nonsteady Combustion in a Solid Propellant Rocket and Predictions of Rocket Motor Stability," (Invited Chapter) To appear in Nonsteady Burning and Combustion Stability of Solid Propellants, Progress in Astronautics and Aeronautics, ed. by L. DeLuca and M. Summerfield.
13. Yang, V. and Culick, F. E. C., "Nonlinear Analysis of Tranverse Pressure Oscillations in Ramjet Engines," AIAA Paper 86-0001, 1986.
14. Kim, S. I., "Nonlinear Combustion Instabilities in Solid Propellant Motors," Ph.D. Thesis, The Pennsylvania State University, 1988.

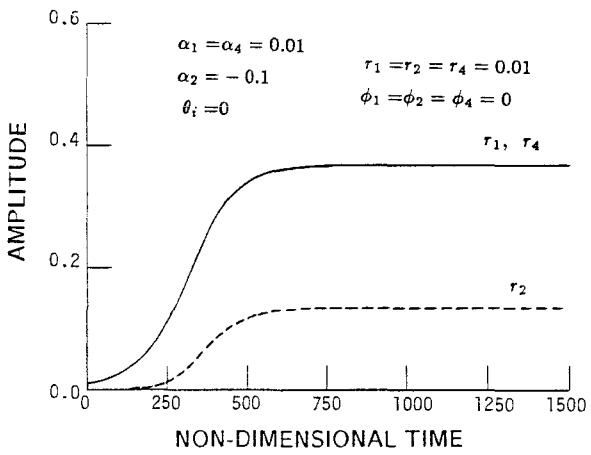

Fig.1 An Example Showing the Existence of a Stable Limit Cycle, 1T/1R Mode.

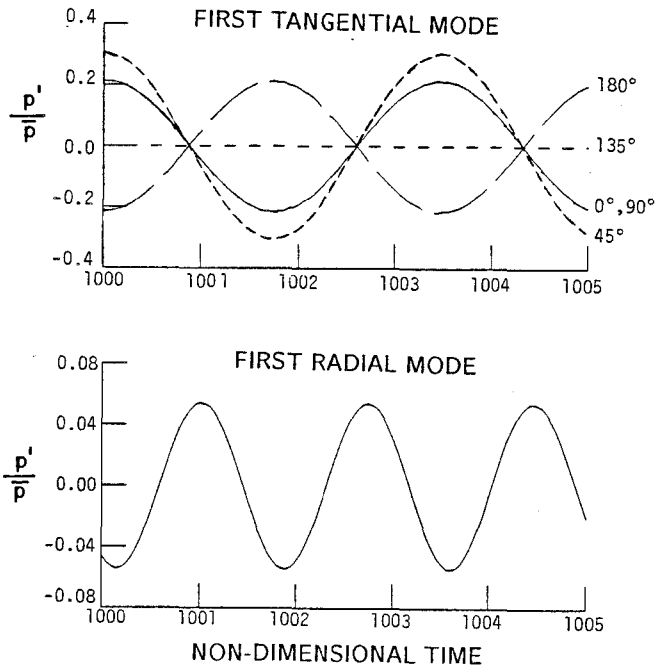

Fig.2 Time Traces of Pressure Oscillations at Various Azimuthal Positions, 1T/1R Mode.

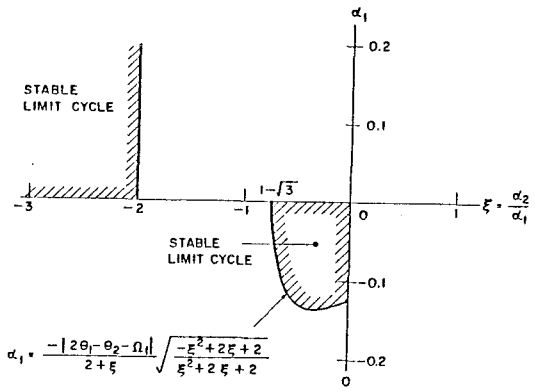

Fig.3 Illustration of the Necessary and Sufficient Conditions for Stable Limit Cycles, $2\theta_1 - \theta_2 - \Omega_1 = 0.25$.

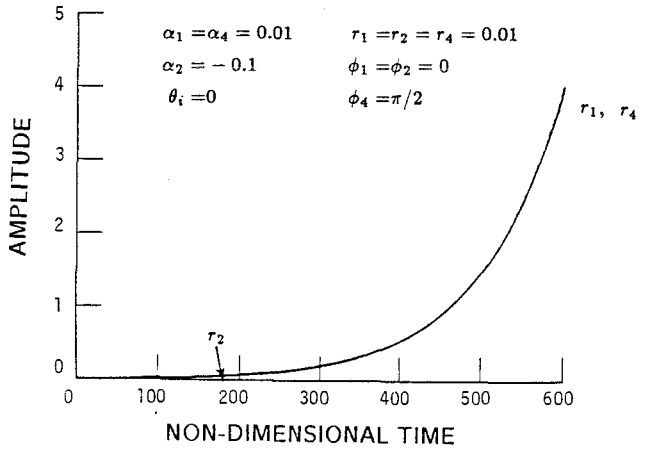

Fig.4 An Example Showing Violation of the Stability Conditions for a Limit Cycle, 1T/1R Mode.

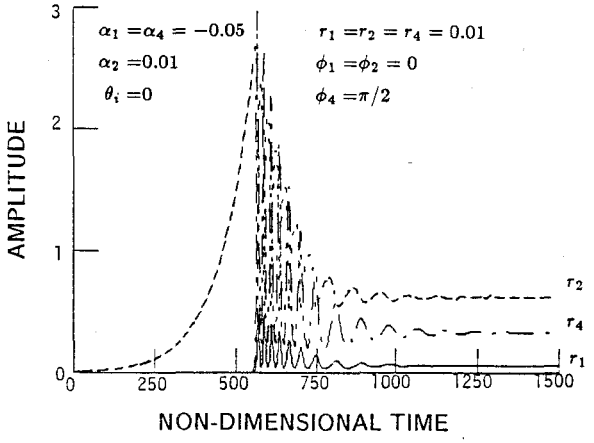

Fig.5 An Example Showing the Existence of a Stable Limit Cycle, 1T/1R Mode.

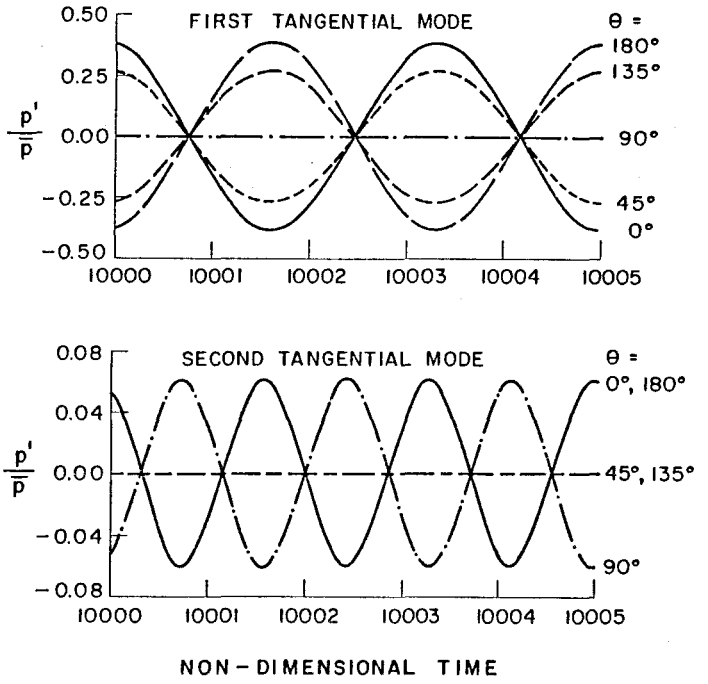

Fig.7 Time Traces of Pressure Oscillations at Various Azimuthal Positions, 1T/2T Mode, Case 1.

$\alpha_1 = 0.01$ $\theta_1 = -0.1$
$\alpha_2 = -0.01$ $\theta_2 = 0.1$
$\alpha_4 = -0.011$ $\theta_4 = -0.2$
$r_1 = r_2 = r_4 = 0.01$
$\phi_1 = \phi_2 = \phi_4 = 0$

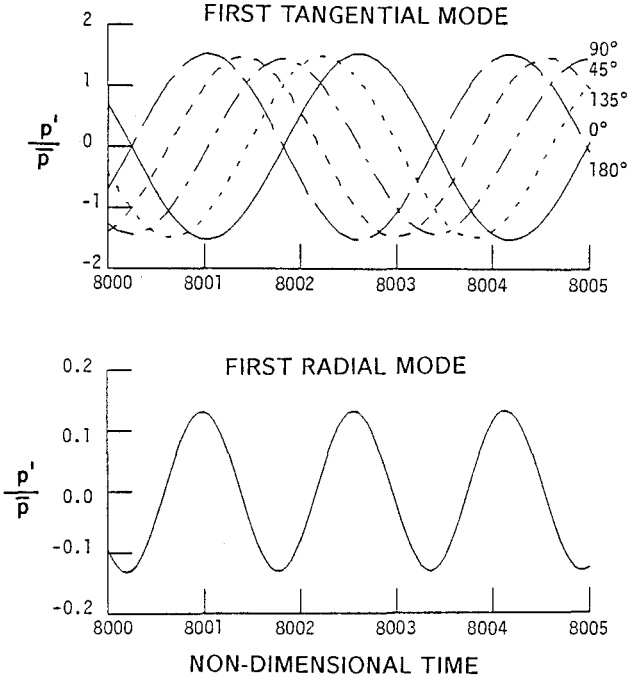

Fig.6 Time Traces of Pressure Oscillations at Various Azimuthal Positions, 1T/1R Mode.

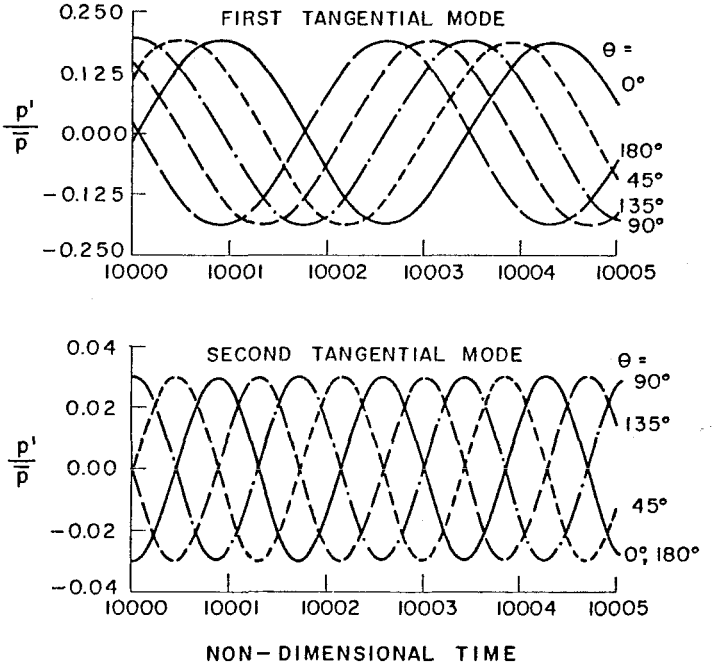

Fig.8 Time Traces of Pressure Oscillations at Various Azimuthal Positions, 1T/2T Mode, Case 2.

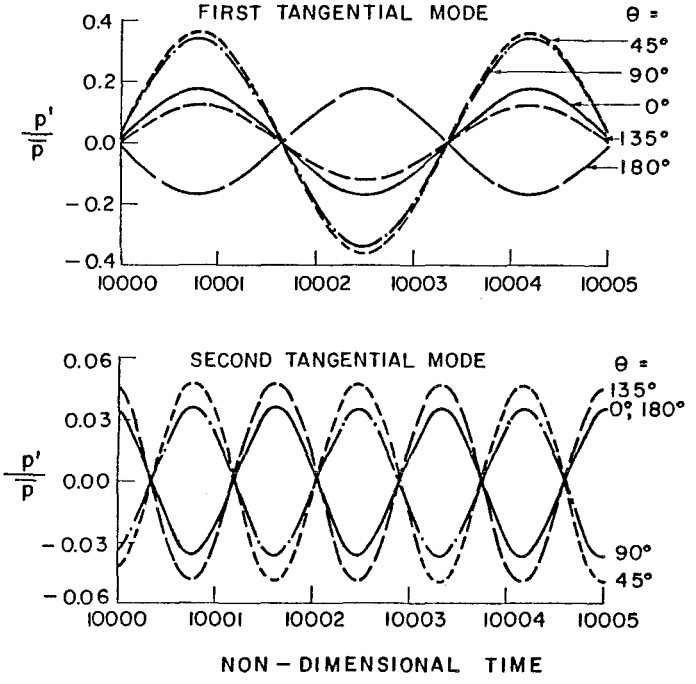

Fig.9 Time Traces of Pressure Oscillations at Various Azimuthal Positions, 1T/2T Mode, Case 3.

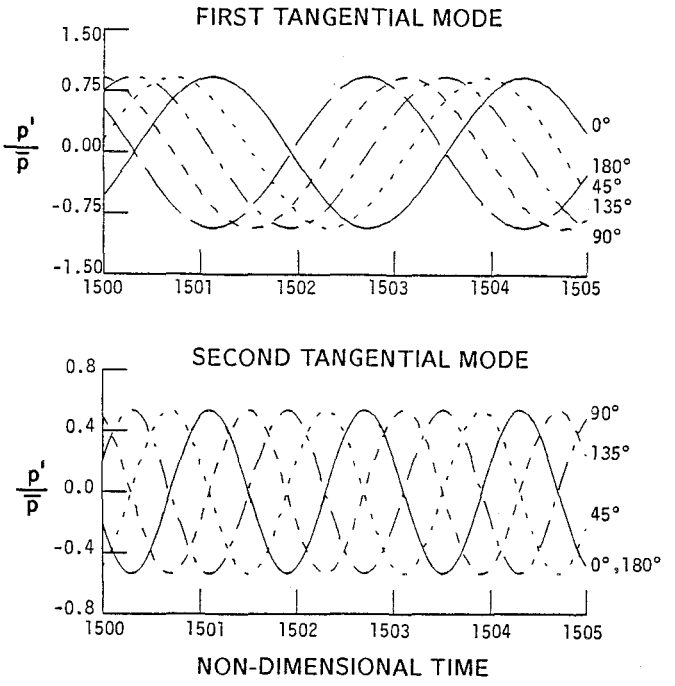

Fig.11 Time Traces of Pressure Oscillations at Various Azimuthal Positions, 1T/1R/2T Mode.

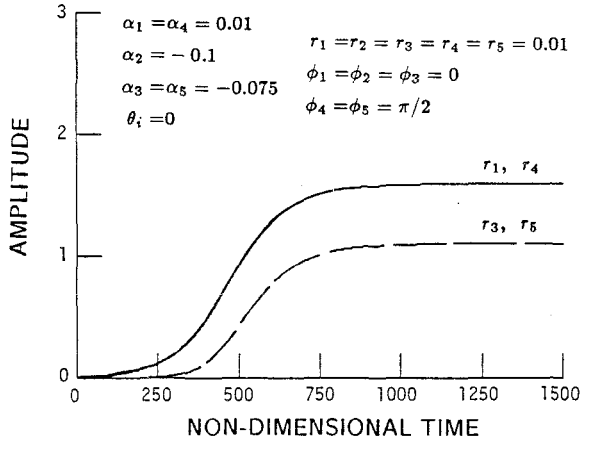

Fig.10 An Example Showing the Existence of a Stable Limit Cycle, 1T/1R/2T Mode.

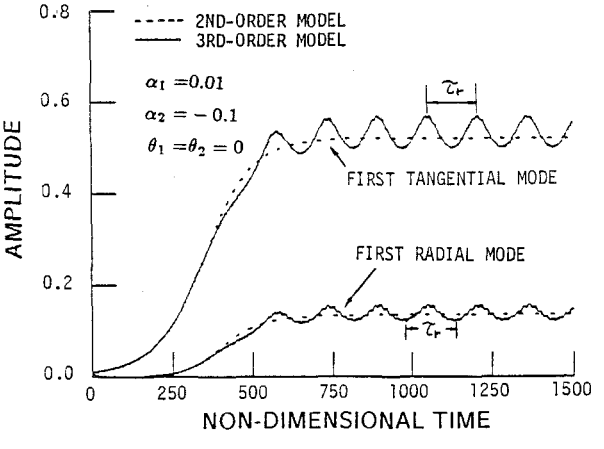

Fig.12 An Example Showing the Existence of a Stable Limit Cycle, 1T/1R Mode.

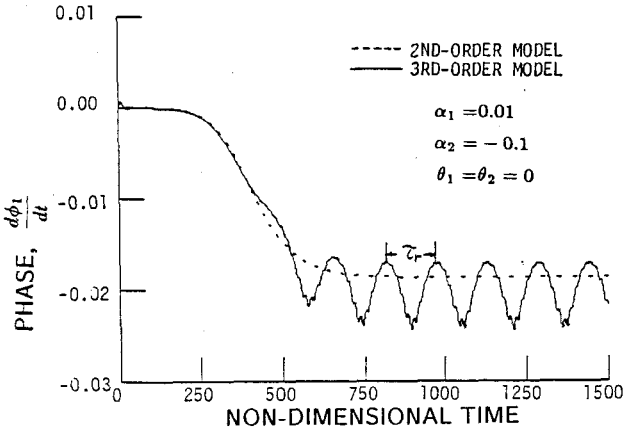

Fig.13a Time History of Phase of the First Tangential Mode, 1T/1R mode.

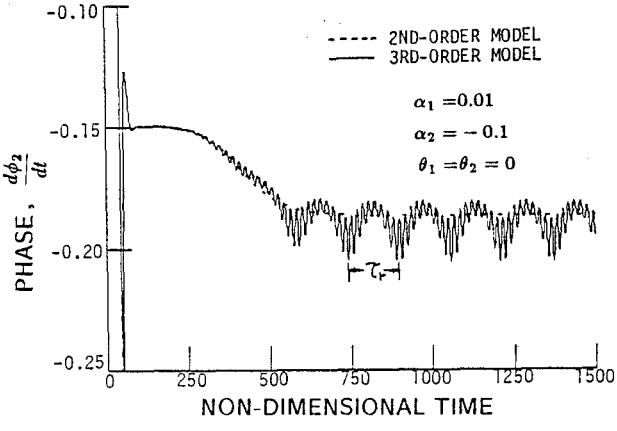

Fig.13b Time History of Phase of the First Radial Mode, 1T/1R mode.

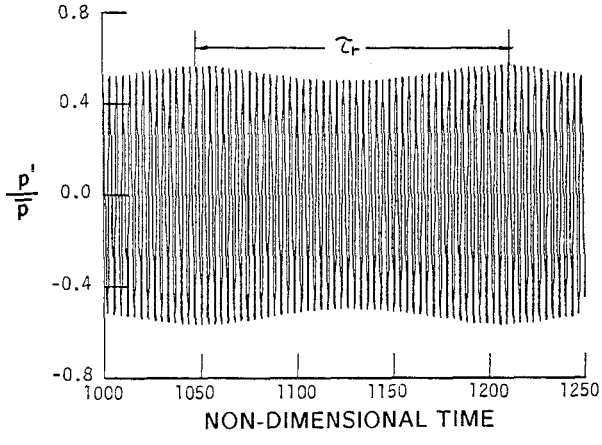

Fig.14a Time Trace of the Amplitude of the First Tangential Mode, 1T/1R mode.

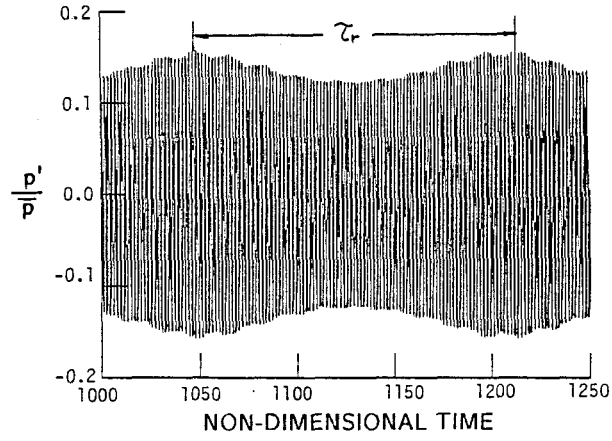

Fig.14b Time Trace of the Amplitude of the First Radial Mode, 1T/1R mode.

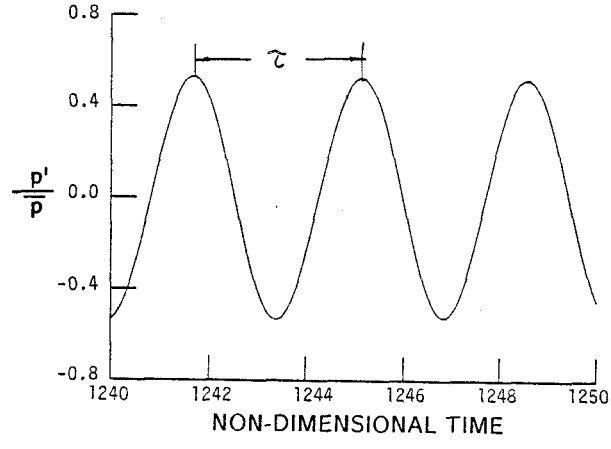

Fig.15a Enlarged Time Trace of the Amplitude of the First Tangential Mode, 1T/1R mode.

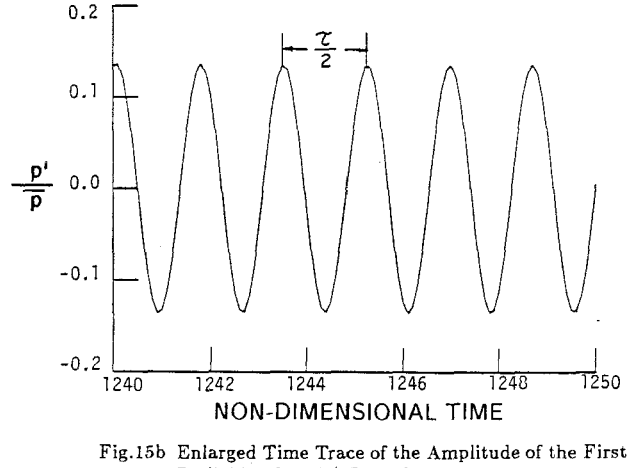

Fig.15b Enlarged Time Trace of the Amplitude of the First Radial Mode, 1T/1R mode.

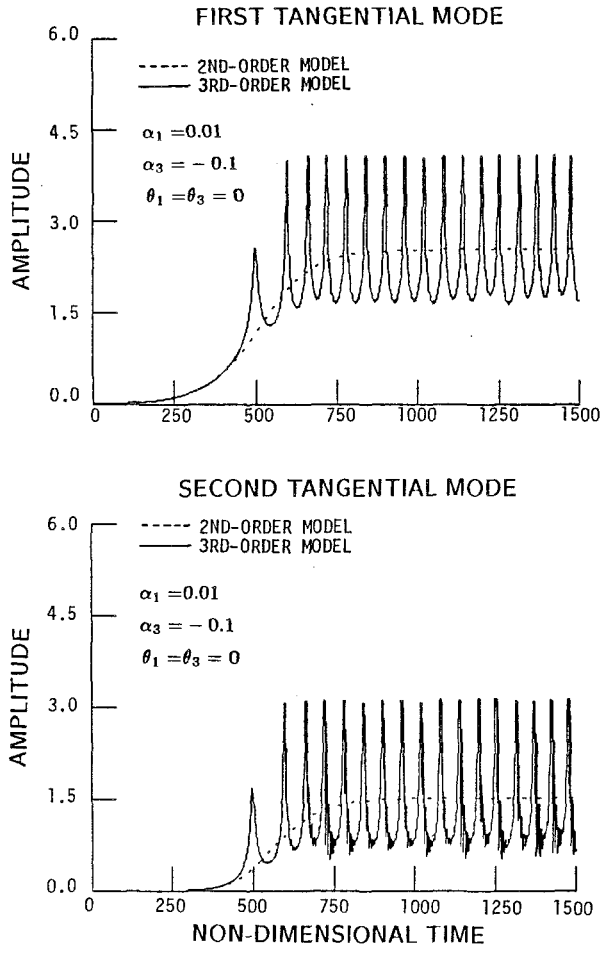

Fig.16 An Example Showing the Existence of a Stable Limit Cycle, 1T/2T Mode.